Isostructural cage complexes of copper with cadmium or zinc for single source deposition of composite materials†

Muhammad Shahid,[a] Muhammad Mazhar,*[a] Mazhar Hamid,[a] Matthias Zeller,[b] Paul O'Brien,*[c] Mohammad A. Malik,[c] James Raftery[c] and Allen D. Hunter[b]

Received (in Victoria, Australia) 25th May 2009, Accepted 23rd July 2009
First published as an Advance Article on the web 20th August 2009
DOI: 10.1039/b9nj00217k

Two heterometallic polynuclear complexes, $[Cd_2(OAc)_6(\mu\text{-}O)Cu_4(dmae)_4]\cdot H_2O$ (**1**) and its zinc analogue $[Zn_2(OAc)_6(\mu\text{-}O)Cu_4(dmae)_4]\cdot 3H_2O$ (**2**), were synthesized by simple chemical techniques. These complexes were characterized by their melting point, elemental analysis, FT-IR, APCI-MS and single crystal X-ray diffraction. The complexes consist of a common Cu_4 moiety and a Cd_2 or Zn_2 moiety in **1** and **2** with the space groups $C2/c$ and $P\bar{1}$, respectively. Thermogravimetric studies prove that they can be easily thermally decomposed and can be used as precursors in aerosol-assisted chemical vapor deposition (AACVD) to yield ceramic composites that might have applications in industry and new technologies. Thin ceramic films thus deposited have good adhesion to the substrate and were characterized by SEM, EDX and powder X-ray diffractometry. SEM micrographs show morphologically evenly distributed phases that were identified by PXRD to be Cu–CdO in the case of **1** and Cu–ZnO for **2**.

Introduction

The properties of "hybrid inorganic materials" are generally controlled by the nature of neighboring atoms or assembled units through weak or strong bonding interactions. The link between individual units is facilitated through the transfer of electrons, ions, photons, alignment of unpaired electrons or local dipole moments.[1] Such types of couplings demand homogeneity at the atomic level[2] which in turn is dependent on the synthetic procedure used for the preparation of the material.

Polynuclear heterometallic complexes are widely used as precursors for chemical vapor deposition (CVD) applications after the emergence of the fact that most of today's high-tech inorganic materials are either bi- or multimetallic oxides. In the past decade, tremendous efforts were directed towards development of homo- and heterobimetallic complexes for their utilization in material transformation.[3–5] Homogeneous distribution of individual atoms on the atomic length scale cannot be achieved by heterogeneous mixing or milling of individual compounds. These mixed bimetallic assemblies are also suitable precursors for the preparation of nanocomposite phases that include the initially blended metals.

Thus, here we are striving to develop heterobimetallic precursors for deposition of thin films of Cu–ZnO and Cu–CdO composites, due to the utility of copper on oxide surfaces in catalysis as well as due to the semiconducting properties of transparent oxides such as ZnO and CdO.[6] The mixed metal–metal-oxide composite Cu–ZnO is the most widely used catalyst for the large scale industrial production of methanol,[7] oxidation of carbon monoxide[8,9] and also Fischer–Tropsch type synthesis.[7]

The solubility of the heterometallic precursor complexes can be enhanced when the central metal–oxygen core is wrapped in a blanket of organic ligands. The presence of organic leaving groups such as amino alcohols and carboxylates in these complexes make them easily pyrolyzable at relatively low temperatures. Thus higher solubility and relatively low pyrolysis temperature make them suitable for liquid based chemical vapour deposition to ceramic materials. Properties such as morphology, particle size, and surface area of the ceramic materials obtained from the heterometallic complexes can be manipulated to some extent by controlling the chamber environment, thermolysis temperature and duration of exposure of substrate to the precursor.[10–12] This method therefore has great potential to tailor properties of ceramic materials for applications in industry.[13]

Experimental section

All manipulations were carried out in a dry argon atmosphere using Schlenk tube and glove box techniques. All solvents and reagents were purchased from Aldrich.

Solvents were rigorously dried and distilled using standard methods. *N*,*N*-Dimethylaminoethanol (dmaeH) was dried by refluxing over K_2CO_3 for 10 h and distilled immediately before use. $Cu(dmae)_2$ was prepared by a literature procedure.[14] Elemental analyses were performed using a CHN Analyzer LECO model CHNS-932. Melting points were determined in a capillary tube using an electrothermal melting point

[a] *Department of Chemistry, Quaid-I-Azam University, Islamabad 45320, Pakistan. E-mail: mazhar42pk@yahoo.com; Fax: +92(0)5190642241; Tel: +92(0)5190642106*
[b] *STaRBURSTT-Cyberdiffraction Consortium at YSU and Department of Chemistry, Youngstown State University, 1 University Plaza, Youngstown, Ohio 44555-3663, USA*
[c] *The School of Chemistry and School of Materials, The University of Manchester, Oxford Road, Manchester, UK M13 9PL. E-mail: paul.obrien@manchester.ac.uk*

† CCDC reference numbers 648033 and 663128. For crystallographic data in CIF or other electronic format see DOI: 10.1039/b9nj00217k

apparatus, model MP.D Mitamura Riken Kogyo (Japan) and are uncorrected. FT-IR spectra were recorded on a single reflectance ATR instrument (4000–400 cm^{-1}, resolution 4 cm^{-1}) from KBr discs. Mass spectra were recorded on a Kratos concept IS instrument. Controlled thermal analyses of the complexes were carried out using a Seiko SSC/S200 thermal analyzer at a heating rate of 10 °C min^{-1} under a N_2 gas flow.

The phase and crystallinity of the deposited films were characterized by means of a Bruker AXS D8 diffractometer using monochromatic Cu-Kα (λ = 0.1541 nm) radiation. A 2θ range of 10.00–90.00° was scanned to cover the diffraction patterns of oxide phases. Surface morphology of the thin films was determined using a FEG-SEM Philips XL30 electron microscope. Samples were carbon coated before observation and EDAX-DX_4 was used to calculate the composition (metallic ratio) of films.

Synthesis of $[Cd_2(OAc)_6(\mu\text{-}O)Cu_4(dmae)_4]\cdot H_2O$ (1)

0.98 g (4.11 mmol) of $Cu(dmae)_2$ was dissolved in THF (20 ml) to make a solution to which 0.80 g (3.00 mmol) $Cd(OAc)_2\cdot 2H_2O$ was added. Three hours of continuous stirring at room temperature, followed by removal of unreacted $Cd(OAc)_2\cdot 2H_2O$ through cannula filtration, gave a shining blue solution. The reaction mixture was evaporated to dryness under vacuum and the solid was redissolved in 10 ml of dichloromethane and crystallized by slow evaporation of the solvent through a septum to give a yield of 75% as a blue crystalline product, m.p. 190 °C. Anal. calc. for $C_{28}H_{60}Cd_2Cu_4N_4O_{18}$: C, 27.57; H, 4.96; N, 4.59%. Found: C, 27.15; H, 5.11; N, 4.19%. FT-IR (KBr, cm^{-1}): 3466br, 2983w, 2876m, 1662s, 1570vs, 1420s, 1342w, 1285w, 1074m, 1016m, 951m, 893m, 786m, 676m, 656w, 608m, 512m, 460w, 432w. APCI-MS (negative scan) *m*/*z*: 1130 [M − (dmae)]$^-$, 1037.2 $[Cu_4(OAc)_5Cd_2(dmae)_3]^-$, 984.2 [M − $(dmae)_2(OAc)]^-$, 865.6 $[Cu_4(OAc)_4Cd(dmae)_3]^-$, 765.7 $[Cu_4(OAc)_2Cd(O)(dmae)_3]^-$, 640.7 $[Cu_3(OAc)Cd(O)(dmae)_3]^-$, 585.1 $[Cu_3(dmae)_3Cd(O)]^-$, 489.7 $[Cu_2(OAc)Cd(O)dmae)_2]^-$, 379.5 $[Cu_2(OAc)(O)(dmae)_2]^-$, 320.7 [M/2 − $Cd(dmae)_2]^-$, 221.3 [M − $Cu_2(OAc)_5Cd_2(dmae)_4]^-$, 157.1 [M − $Cu_3(OAc)_5Cd_2(dmae)_4]^-$. TGA: 112–242 °C (41 wt% loss), 242–289 °C (13.8 wt% loss), 289–503 °C (residue of 40.5%).

Synthesis of $[Zn_2(OAc)_6(\mu\text{-}O)Cu_4(dmae)_4]\cdot 3H_2O$ (2)

0.15 g (4.80 mmol) of $Cu(dmae)_2$ was dissolved in 15 ml THF. The dark pink solution thus obtained was transferred to a 100 ml Schlenk tube containing a stirring suspension of 0.80 g (3.65 mmol) $Zn(OAc)_2\cdot 2H_2O$ in 10 ml THF. The reaction mixture was allowed to stir for 3 h at room temperature. The resulting blue solution was filtered through a cannula and evaporated to dryness under vacuum to eliminate volatiles. The solid was redissolved in a minimum amount of THF and was allowed to stand for crystallization under an inert atmosphere to give a 70% yield of blue crystals of **2** at −10 °C after three weeks, m.p. 135 °C. Anal. calc. for $C_{28}H_{64}Cu_4Zn_2N_4O_{20}$: C, 29.1; H, 5.06; N, 4.85%. Found: C, 29.01; H, 5.47; N, 4.67%. FT-IR (KBr, cm^{-1}): 3435br, 2977w, 2891m, 1667s, 1568vs, 1413s, 1341m, 1193w, 1068m, 1018m, 952m, 896w, 784w, 679m, 617m, 523w, 461w, 428w. APCI-MS (negative scan) *m*/*z*: 1159.5 [M]$^-$, 1059.1 $[Cu_3(dmae)_4(O)_2Zn_2(OAc)_6]^-$, 1033.6 $[Cu_4(dmae)_3(O)_2Zn_2(OAc)_6]^-$, 953.1 $[Cu_4(dmae)_3(O)Zn(OAc)_6]^-$, 929 $[Cu_3(dmae)_4(O)_2(OAc)_6]^-$, 896.4 $[Cu_3(dmae)_3(O)Zn_2(OAc)_5]^-$, 832.7 $[Cu_2(dmae)_3(O)Zn_2(OAc)_5]^-$, 775.2 $[Cu_2(dmae)_3(O)Zn_2(OAc)_4]^-$, 752 $[Cu_2(dmae)_3Zn(OAc)_4]^-$, 669.3 $[Cu_2(dmae)_2Zn_2(OAc)_4]^-$, 667.3 $[Cu_3(dmae)_2Zn(OAc)_4]^-$, 638.5 $[Cu_3(dmae)Zn(OAc)_5]^-$, 636.2 $[Cu_4(dmae)(OAc)_5]^-$, 518.7 $[Cu(dmae)Zn_2(OAc)_4]^-$, 512.5 $[Cu(dmae)Zn(OAc)_5]^-$, 483.1 $[Cu(OAc)_6Zn]^-$, 414.2 $[Cu(dmae)(O)Zn_2(OAc)_2]^-$, 288.9 $[Zn(dmae)(O)(OAc)_2]^-$, 228.6 $[Zn(dmae)(O)(OAc)]^-$. TGA: 89–190 °C (4.84 wt% loss), 190–280 °C (58.05 wt% loss), 280–440 °C (residue of 34.9%).

X-Ray crystallography

Single crystal diffraction data of complexes **1** and **2** were collected on Bruker AXS SMART APEX CCD diffractometers at 100(2) K using monochromatic Mo-Kα radiation with omega scan technique. The structures were solved by direct methods[15] and refined by full-matrix least-squares against F^2 with all reflections using SHELXTL.[16] Refinement of extinction coefficients was found to be insignificant. All non-hydrogen atoms were refined anisotropically. In **1**, one of the dmae ligands was found to be disordered by a pseudo-mirror operation over two positions with an occupancy ratio of 0.68(1) : 0.32(1). In **2**, three of the dmae ligands were found to be disordered in a similar fashion over each of two positions with occupancies for the major moieties of 0.504(8), 0.741(5) and 0.6774(7). Chemically equivalent bonds in disordered sections of **1** and **2** were each restrained to be the same within a standard deviation of 0.02 Å and equivalent atoms were constrained to have identical ADPs. The water hydrogen atoms were set geometrically so as to fit with the expected hydrogen bonding pattern. All other hydrogen atoms in **1** and **2** were placed in calculated positions and were refined with an isotropic displacement parameter of 1.5 (methyl) or 1.2 (all others) times that of the adjacent carbon atom. Table 1 summarizes the crystal data and refinement details for both complexes.

Deposition of thin films

Cu–CdO and Cu–ZnO composite thin films were deposited on a soda glass substrate in a hot walled reactor by gas phase reactions of the precursors in an argon environment at atmospheric pressure using a self-designed aerosol-assisted chemical vapor deposition (AACVD) assembly described elsewhere.[17] In a typical experiment, 0.1 g of precursor dissolved in 10 ml toluene and 5 ml dichloromethane in a two neck round bottomed flask was connected *via* rubber tubing to a quartz reactor loaded with 2.5 × 1 cm substrate slides inside a carbolite tube furnace. The flow of argon gas was regulated using a Platon flow gauge on the other neck. The flask was fitted on an ultrasonic humidifier equipped with a piezoelectric modulator for atomization of the precursor solution into tiny droplets of aerosol that were ultimately transferred by the carrier gas into the reactor chamber. Glass substrates were washed with concentrated nitric acid, followed by washing several times with deionized water and then oven dried at 100 °C. Deposition on substrates was carried out at 500 °C for

Table 1 Crystal data and refinement parameters for the complex $[Cd_2(OAc)_6(\mu\text{-}O)Cu_4(dmae)_4]\cdot H_2O$ (**1**) and $[Zn_2(OAc)_6(\mu\text{-}O)Cu_4(dmae)_4]\cdot 3H_2O$ (**2**)

Empirical formula	$C_{28}H_{60}Cd_2Cu_4N_4O_{18}$	$C_{28}H_{64}Zn_2Cu_4N_4O_{20}$
Formula weight	1219.76	1161.73
Temperature	100(2) K	100(2) K
Wavelength	0.71073 Å	0.71073 Å
Crystal system	Monoclinic	Triclinic
Space group	$C2/c$	$P\bar{1}$
Unit cell dimensions	a = 21.449(3) Å, b = 13.6325(16) Å, c = 15.8019(18) Å $\alpha = \gamma = 90°$, β = 108.779(2)°	a = 12.2838(12) Å, b = 13.3453(13) Å, c = 13.6289(13) Å α = 83.401(2)°, β = 84.511(2)°, γ = 79.691(2)°
Volume	4374.6(9) Å^3	2177.1(4) Å^3
Z	4	2
Density (calculated)	1.852 Mg m^{-3}	1.772 Mg m^{-3}
Absorption coefficient	2.935 mm^{-1}	3.080 mm^{-1}
$F(000)$	2448	1192
Crystal size	0.50 × 0.31 × 0.10 mm	0.20 × 0.15 × 0.10 mm
θ range for data collection	1.80 to 28.30°	1.51 to 28.30°
Index ranges	$-28 \le h \le 27$, $-18 \le k \le 17$, $-20 \le l \le 21$	$-16 \le h \le 16$, $-17 \le k \le 17$, $-17 \le l \le 17$
Reflections collected	16 902	19 171
Independent reflections	5376 [R(int) = 0.0335]	9954 [R(int) = 0.0691]
Max. and min. transmission	0.746 and 0.384	0.7482 and 0.5779
Refinement method	Full-matrix least-squares on F^2	Full-matrix least-squares on F^2
Goodness-of-fit on F^2	1.214	0.803
Final R indices [$I > 2\sigma(I)$]	$R1$ = 0.0627, w$R2$ = 0.1381	$R1$ = 0.0391, w$R2$ = 0.0724
R indices (all data)	$R1$ = 0.1028, w$R2$ = 0.1803	$R1$ = 0.0706, w$R2$ = 0.0797
Largest diff. peak and hole	2.459 and −1.388 e Å^{-3}	0.60 and −0.76 e Å^{-3}

complex **1** and 450 °C for **2** at a constant argon flow rate of 130 ml min^{-1} for 2.5 h.

Results and discussion

For the synthesis of both compounds, the same synthetic strategy was used. For **1**, $Cu(dmae)_2$ was reacted with $Cd(OAc)_2{\cdot}2H_2O$, and with $Zn(OAc)_2{\cdot}2H_2O$ for **2** as indicated in the following reaction scheme.

$$3M(OAc)_2\cdot 2H_2O + 4Cu(dmae)_2 \xrightarrow{THF} M_2(OAc)_6(\mu\text{-}O)Cu_4(dmae)_4\cdot xH_2O + M(dmae)_2 + 2dmaeH + yH_2O$$

$$M = Cd,\ x = 1,\ y = 4\ (\mathbf{1}) : M = Zn,\ x = 3,\ y = 2\ (\mathbf{2})$$

Both complexes are stable under ordinary conditions, soluble in common organic solvents, volatile and are used as single source bimetallic precursors for deposition of mixed M–M'O composite materials through the AACVD technique.

The structural features of both complexes were determined by elemental analysis, FT-IR spectroscopy, mass spectrometry and finally confirmed by single crystal X-ray diffraction studies. In the FT-IR spectra, the broad absorption band at 3466 cm^{-1} due to the water molecule present in complex **1** is at a slightly higher frequency than the O–H absorption band in complex **2** at 3435 cm^{-1}. Reported infrared data for carboxylate complexes in the frequency range 1410–1670 cm^{-1} suggested the presence of different coordination modes for the acetate ligands[18] for both complexes. Definite absorption frequencies could however not be assigned. The absorptions at lower frequency (512–523 cm^{-1}) are due to ν(Cu–O) vibrations, while the absorption bands in the range 428–461 cm^{-1} are assigned to ν(M–N) vibrations in both cases.[19] APCI mass spectra (negative scan) of complex **1** did not show a molecular ion peak but the fragments of different m/z ratios indicating the formation of the complex were found. The largest fragment observed is $[M - (dmae)]^-$ at m/z (1130), with the base peak at m/z (865.6) corresponding to $[Cu_4(OAc)_4Cd(dmae)_3]^-$. On the other hand, APCI mass spectra (negative scan) of complex **2** exhibits the molecular ion as well as fragment ion peaks (having different m/z ratios) with the peak of maximum intensity at m/z (667.3) for $[Cu_3(dmae)_2Zn(OAc)_4]^-$, thus showing the stability of the complex under the MS conditions.

Complexes **1** and **2** crystallize in different settings, monoclinic C centered and triclinic, and with a different water content. Crystal structure data and refinement parameters for both compounds are given in Table 1 and the selected metrical data are tabulated in Table 2 and 3, respectively. The single crystal diffraction data show however that the individual molecules of the two compounds are closely related. Both **1** and **2** are hexanuclear complexes that are made up of two triangular MCu_2 units (where M = Cd or Zn) which are linked by four dmae μ_3-alkoxo and one μ_4-oxo bridges. In complex **1**, the molecule is located on a two-fold crystallographic axis. Complex **2** is located on a general site with no crystallographic symmetry. Cu(1) of complex **1** is analogous to Cu(1) and Cu(1A) of **2**, Cu(2) to Cu(2) and Cu(2A), and Cd1 to Zn1 and Zn1A, respectively. Both complexes are very similar except for the substitution of cadmium by zinc and the presence of two more solvate water molecules for **2** with only minor differences in their respective bond lengths, angles and ligand coordination types. Structural details are thus

Table 2 Selected metrical data for complex **1**[a]

Bond distances (Å)			
Cu(1)–O(3)	1.910(5)	Cu(2)–N(1)	2.027(7)
Cu(1)–O(1)	1.954(3)	Cu(2)–O(3)	2.423(5)
Cu(1)–O(4)	2.429(6)	Cd(1)–O(5)	2.232(5)
Cu(1)–Cu(2)	2.904(13)	Cd(1)–O(3)	2.272(6)
Cu(2)–O(2)	1.954(5)	Cd(1)–O(2)	2.299(5)
Cu(2)–O(1)	1.966(2)	Cd(1)–O(6)	2.357(6)
Cu(2)–O(4)^{i}	2.548(5)	Cd(1)–O(7)	2.412(6)
Bond angles (°)			
O(3)–Cu(1)–O(1)	86.9(2)	O(2)–Cu(2)–N(1)	85.1(3)
O(9)–Cu(1)–O(1)	95.7(2)	N(1)–Cu(2)–O(3)	103.8(2)
O(3)–Cu(1)–N(2)	86.9(2)	O(5)–Cd(1)–O(3)	95.1(2)
O(1)–Cu(1)–N(2)	167.10(19)	O(3)–Cd(1)–O(2)	83.25(18)
O(3)–Cu(1)–O(4)	92.3(2)	O(2)–Cd(1)–O(2)	76.5(2)
N(2)–Cu(1)–O(4)	97.8(2)	O(3)–Cd(1)–O(6)	143.6(2)
O(1)–Cu(2)–O(3)	73.74(13)	O(2)–Cd(1)–O(6)	97.0(2)

[a] Symmetry operator *i*: $-x + 1, y, -z + 1/2$.

discussed for the cadmium complex only (Fig. 1) and compared with those of the zinc complex (Fig. 2), wherever necessary.

The four dmae μ_3-oxygen atoms, O(2), O(2A), O(3) and O(3A), act as chelating bridging connectors that link the six heterometallic centers. The μ_4-oxygen atom O(1) is surrounded by four copper atoms in a distorted tetrahedral manner. The acetate ligands in both complexes coordinate in a variety of coordination modes. They are either chelating [O(6), O(7); O(6A), O(7A)], bridging [O(8), O(9); O(8A), O(9A)] or bridging bidentate [through O(4), O(5); O(4A), O(5A)] and bridging unidentate [through O(4) and O(4A)]. The intermetallic distances in the complex *i.e.*, Cu···Cu, Cu···Cd and Cd···Cd are in the range 2.904–3.796, 3.348–4.891 and 3.602 Å, respectively, which suggests that no metal–metal bonds are formed.

The Cu(1) atom in complex **1** is in a slightly distorted square pyramidal environment (Fig. 3) consisting of N(2) and O(3) of a chelating bridging dmae ligand, O(9) of a bridging acetate, and μ_4-oxygen atom O(1) forming the basal plane with the oxygen atom O(4) of a bridging bidentate acetate group occupying the apical position. The copper–oxygen bond distance of Cu(1) to the apical oxygen atom O(4) is much

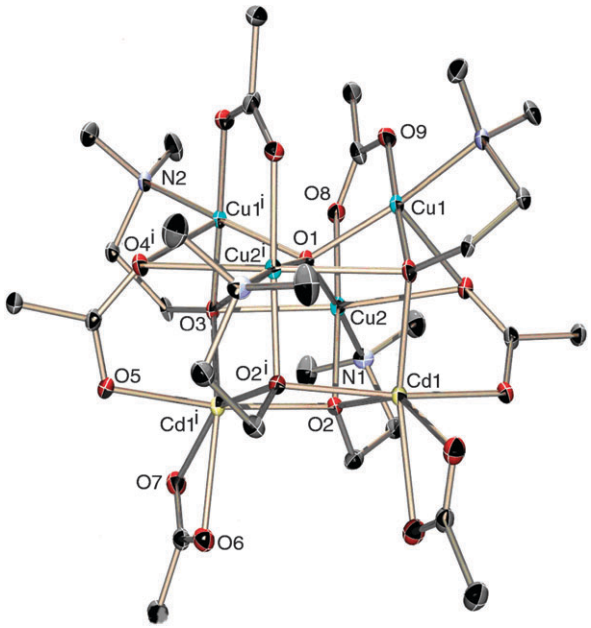

Fig. 1 Simplified ORTEP drawing showing the molecular structure of $[Cd_2(OAc)_6(\mu\text{-}O)Cu_4(dmae)_4]\cdot H_2O$ (**1**). All hydrogen atoms and water molecules as well as minor disordered moieties are omitted for clarity. Thermal ellipsoids are at the 30% level [symmetry operator *i*: $-x + 1, y, -z + 1/2$].

longer [2.429(6) Å] than all other Cu–O bond lengths around Cu(1) which range from 1.910(5) to 1.954(3) Å and are close in value to the sum of the ionic radii, 1.92 Å. The Cu(2) metal center adopts a tetragonally elongated octahedral coordination with Cu–O/N bond lengths in the basal plane ranging from 1.954(5) to 2.027(7) Å and weaker apical bonds to oxygen atoms [O(3) and O(4) of a chelating bridging dmae ligand and a bridging bidentate acetate group, respectively] in the range of 2.423(5)–2.548(5) Å (Table 2).

Both the Cd atoms are six coordinate; the coordination sphere consists of two oxygen atoms [O(6), O(7)] of a chelating acetate, one oxygen atom [O(5)] of a bridging

Table 3 Selected metrical data for complex **2**

Bond distances (Å)			
Cu(1A)–O(3)	1.938(3)	Cu(2)–Zn(1)	3.1318(8)
Cu(1A)–O(1)	1.950(3)	Cu(2)–O(4A)	2.397(3)
Cu(1A)–O(8)	2.323(3)	Zn(1)–O(3)	2.060(3)
Cu(1A)–Cu(2A)	2.906(8)	Zn(1)–O(7)	2.524(3)
Cu(1A)–Zn(1A)	3.2082(8)	Zn(1)–O(5)	2.036(3)
Cu(2)–O(1)	1.955(3)	Zn(1)–O(6)	2.100(3)
Cu(2)–O(2)	1.971(3)	Zn(1A)–O(2)	2.101(3)
Cu(2)–N(1)	2.052(4)	Zn(1A)–O(2A)	2.136(3)
Cu(2)–O(3)	2.431(3)		
Bond angles (°)			
O(1)–Cu(1A)–O(3A)	86.05(11)	O(6)–Zn(1)–O(3)	138.98(12)
O(1)–Cu(1A)–O(9)	93.67(12)	O(6)–Zn(1)–O(2)	93.46(11)
O(3A)–Cu(1A)–N(2A)	86.81(13)	O(3)–Zn(1)–O(2A)	119.13(11)
O(1)–Cu(1A)–N(2A)	165.27(13)	O(2)–Zn(1)–O(2A)	78.18(11)
O(3A)–Cu(1A)–O(4A)	94.61(11)	O(5A)–Zn(1A)–O(3A)	91.67(12)
N(2A)–Cu(1A)–O(4A)	99.25(12)	O(3A)–Zn(1A)–O(6A)	130.85(12)
O(2)–Cu(2)–N(1)	85.40(13)	O(2)–Zn(1A)–O(6A)	106.76(11)
O(1)–Cu(2)–O(3)	72.54(10)	O(3A)–Zn(1A)–O(2A)	87.36(11)
N(1)–Cu(2)–O(3)	104.03(12)	O(2)–Zn(1A)–O(2A)	78.02(10)

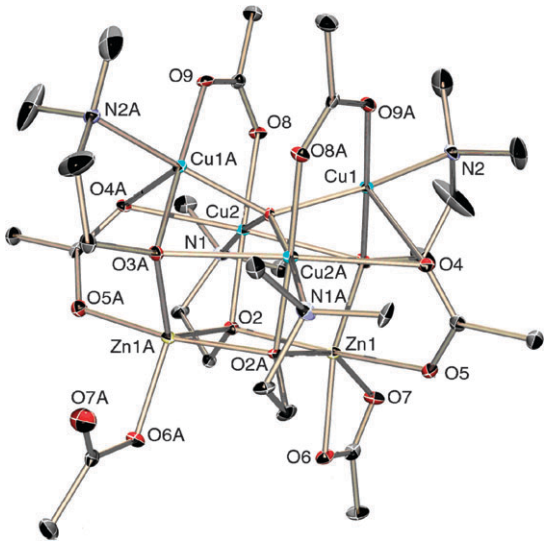

Fig. 2 An ORTEP plot of the molecular structure of $[Zn_2(OAc)_6(\mu\text{-}O)(Cu_4dmae)_4]\cdot 3H_2O$ (**2**) (Atoms labeled 'A' are chemically related to unlabeled atoms, but not crystallographically). All hydrogen atoms and water molecules as well as minor disordered moieties are omitted for clarity. Thermal ellipsoids are at the 30% level.

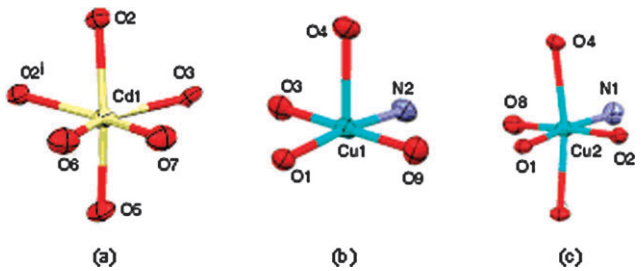

Fig. 3 Geometric spheres of (a) octahedral Cd(1), (b) square pyramidal Cu(1) and (c) octahedral Cu(2) in **1**[symmetry operator *i*: $-x + 1, y, -z + 1/2$].

bidentate acetate group and three oxygen atoms [O(2), O(2A), O(3)] of chelating bridging dmae ligands forming a CdO_6 distorted octahedron with bond lengths in the range 2.232(5)–2.412(6) Å (Table 2) which is coherent with the literature.[20–22] The observed coordination modes are in agreement with those found in $Cd(O_2CMe)_2(H_2O)_2$, $Cu(O_2CMe)$ and $[Cd(O_2CMe)_2(H_2O)]_2$.[18]

In contrast to **1**, the two zinc atoms in **2** are distinct. Zn(1) has a distorted octahedral geometry with a ZnO_6 core similar to Cd atoms in complex **1**, while Zn(1A) is in a trigonal bipyramidal environment because one of the acetate groups attached to it is coordinating in a monodentate fashion instead of in a bidentate chelating mode as found for Zn(1). The coordination sphere of Zn(1A) (Fig. 4) comprises three oxygen atoms O(2), O(2A) and O(3A) [O(2) and O(2A) link Zn(1A) with Zn(1) resulting in a four membered Zn_2O_2 ring, while O(3A) connects it with Cu(1A) and Cu(2A) with a separation of 3.2082(8) and 3.105(6) Å, respectively] of dmae ligands, one oxygen atom O(5A) of a bridging acetate and an oxygen atom O(6A) of a monodentate acetate group.

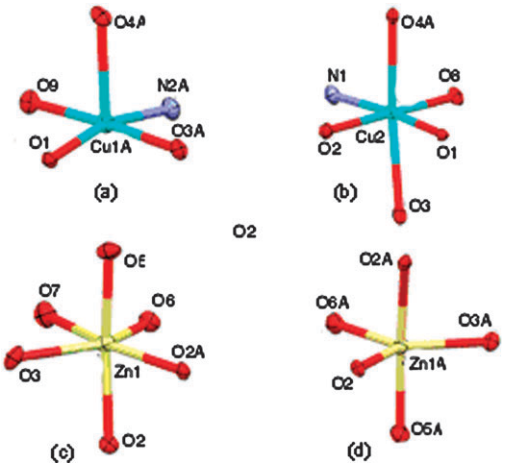

Fig. 4 Coordination spheres of metal centers in **2**, (a) square pyramidal Cu(1A) ≃ Cu1, (b) octahedral Cu(2) ≃ Cu(2A), (c) octahedral Zn(1) and (d) trigonal bipyramidal Zn(1A).

Additional stability for complex **1** is provided by intermolecular hydrogen bonding [O(10)–H(10D)···O(6)] between oxygen atom O(6) of a chelating acetate group and hydrogen atom H(10D) of the water molecule which is present in the crystal structure as water of hydration. Similar hydrogen bonding interactions are also found in complex (**2**). Here the three crystallographically independent water molecules are also involved in hydrogen bonds with each other.

Thermogravimetric studies

The thermal behavior of complexes **1** and **2** was studied by thermogravimetric analysis over the temperature range 25–550 °C at a scanning rate of 10 °C min^{-1} in a nitrogen (130 ml min^{-1}) environment (Fig. 5). The TGA curve of **1** demonstrates a three stage decomposition pattern. The first stage starts at 112 °C and is completed at 242 °C with a weight loss of 41%. The second weight loss (13.8%) takes place between 242–289 °C which is directly followed by the last step ranging from 289 °C to 503 °C, resulting in a residue of 40.5% of the initial weight. The residual weight (40.5%) is slightly less but comparable to 41.9%, calculated for complete decomposition of **1** to a residue of the composition (4Cu + 2CdO). The

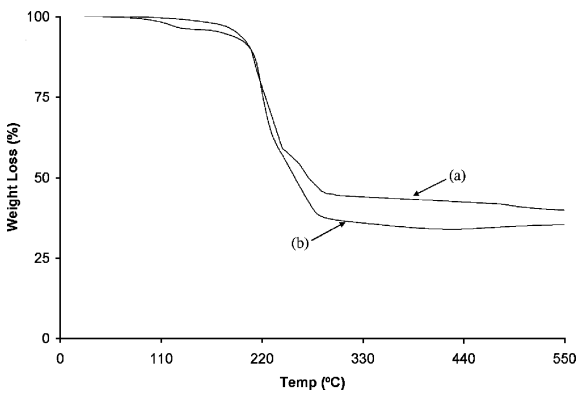

Fig. 5 Thermogravimetric plot showing the loss in weight with the rise in temperature for (a) complex **1** and (b) **2**.

TGA plot of **2** also shows three steps of weight loss. The decomposition begins at 89 °C and completes at 440 °C, with maximum weight loss (58.05%) between 189–280 °C, leaving a residue of 34.9% of the initial weight. The residual mass (34.9%) is again slightly less but close to the expected composition of (4Cu + 2ZnO). The presence of such a (4Cu + 2MO) composite (with M = Cd or Zn) was further supported by PXRD analysis of the thin films. TGA studies of **1** and **2** demonstrate an almost quantitative decomposition of complexes to the proposed composites with poor sublimation properties.

Thin film studies

Thin films of mixed-metal oxides were prepared from **1** and **2** at 500 and 450 °C, respectively, using a customized AACVD assembly. Glass slides were placed horizontal to the aerosol thrust in a silica tube fitted in a hot walled tube reactor. This arrangement ensures a uniform film deposition with maximum covered area. Films were studied and characterized for their surface morphology, metallic composition and distribution by SEM/EDX. The nature of the crystalline phases was investigated by PXRD. Physically, both the thin films are reflecting light in multi-shaded fringes, are stable towards air and moisture and qualify in the "scotch-tape test" indicating good adhesion to the substrate.

A scanning electron microscopic (SEM) image (Fig. 6) of a Cu–CdO composite thin film deposited from complex **1** at 450 °C shows a highly compact and smooth film morphology with homogeneously dispersed particles. The particle size falls in the range of 0.3–0.7 μm and the particles have variable shapes. A SEM image (Fig. 7) of a Cu–ZnO composite thin film obtained from complex **2** shows a film morphology consisting of spherical grains of different sizes, uniformly dispersed throughout the film. The particles with a size range of 0.3–0.6 μm have well-defined boundaries. Energy dispersive X-ray analysis indicates that the ratio of Cu : Cd in complex **1** and Cu : Zn in complex **2** is close to 2 : 1 (atomic ratio Cu, 31.15 : Cd, 16 for **1** and Cu, 31.24 : Zn, 15.98 for **2**) which confirms the retention of the same metallic ratio in the films as in the complexes.

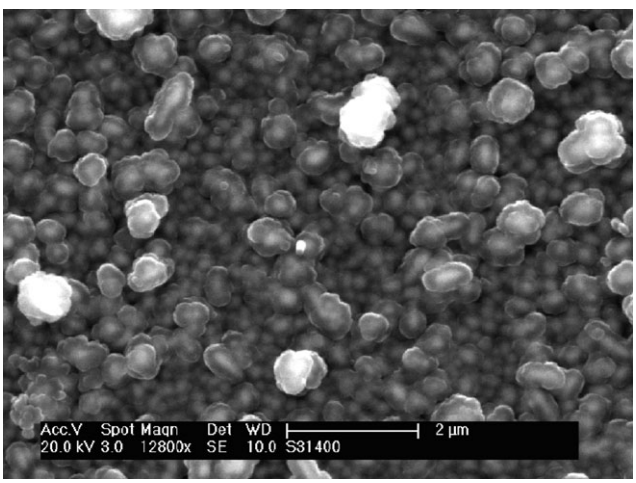

Fig. 6 SEM micrograph of Cu–CdO composite films deposited from complex **1** at 500 °C by AACVD method.

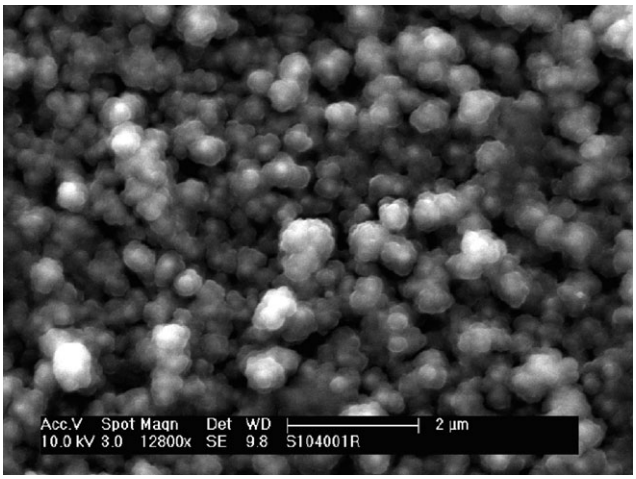

Fig. 7 SEM micrograph of Cu–ZnO composite films deposited from complex **2** at 450 °C by AACVD method.

The X-ray diffractograms of the films obtained from complexes **1** and **2** (Fig. 8 and 9) indicate the formation of Cu–CdO and Cu–ZnO composites, respectively according to the following equations.

$$M_2(OAc)_6(\mu\text{-}O)Cu_4(dmae)_4 \cdot xH_2O \xrightarrow[450-500^\circ C]{AACVD} 2MO + 4Cu + \text{Volatiles}$$

$$M = Cd,\ x = 1\ (\mathbf{1}); M = Zn,\ x = 3\ (\mathbf{2})$$

In the case of complex **1**, the XRD peak pattern indicates the presence of CdO[23] and Cu metal.[24] Both crystalline phases (CdO and Cu) are in cubic space group $Fm\bar{3}m$, while in the case of **2**, the phases identified are ZnO[25] and again Cu metal[24] having hexagonal and cubic crystal systems with space groups $P6_3mc$ and $Fm\bar{3}m$, respectively. Powder X-ray diffractograms of the films fabricated from both the complexes also show that the ZnO phase deposited in the case of precursor **2** is highly crystalline whereas the CdO phase obtained from **1** has a relatively lower crystallinity.

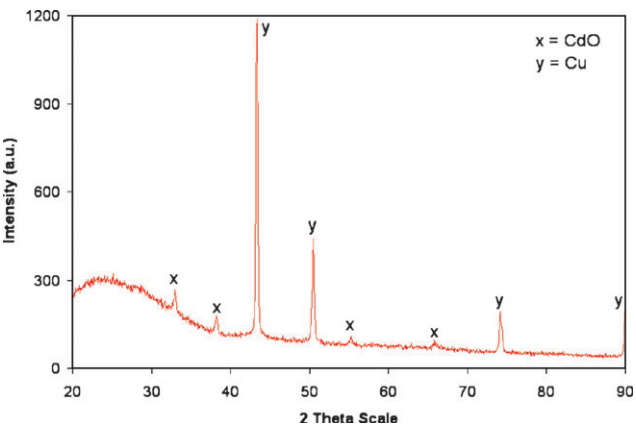

Fig. 8 X-Ray diffractogram of Cu–CdO films deposited from complex **1** at 500 °C, x = CdO [01-073-2245] and y = Cu [01-089-2838].

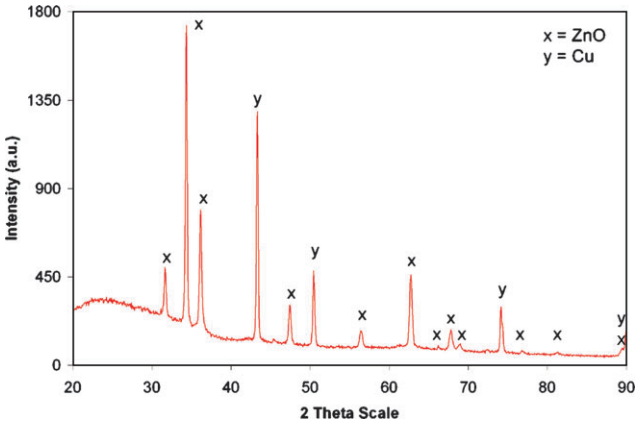

Fig. 9 X-Ray diffractogram of Cu–ZnO films deposited from complex **2** at 450 °C, x = ZnO [01-079-0208] and y = Cu [01-089-2838].

Conclusion

The synthesis of isostructural heterobimetallic complexes $[Cd_2(OAc)_6(\mu\text{-}O)Cu_4(dmae)_4]\cdot H_2O$ (**1**) and $[Zn_2(OAc)_6(\mu\text{-}O)\text{-}Cu_4(dmae)_4]\cdot 3H_2O$ (**2**) can be carried out by a routine chemical approach and the compounds were characterized by physical and spectroscopic techniques. The pyrolysis patterns of both the complexes indicate the facile decomposition of the complexes at relatively low temperature, which makes them ideal for the growth of composite materials by the AACVD method. The deposited thin films, characterized by SEM, EDX and XRD show good quality, a smooth morphology and uniform distribution with Cu : MO ratios close to 2 : 1 (where M = Zn or Cd).

Acknowledgements

M.S. and M.M. would like to thank the Higher Education Commission, Islamabad, Pakistan for financial support through the "Indigenous 5000 and open merit 200 PhD Scholarship Scheme" and the Pakistan Science Foundation through project PSF/RES/C-QU/CHEM(408). The diffractometer at YSU was funded by NSF grant 0087210, by Ohio Board of Regents grant CAP-491, and by YSU.

Notes and references

1 K. O. Caulton and L. G. Hubert-Pfalzgraf, *Chem. Rev.*, 1990, **90**, 969.
2 H. Dislich, *Angew. Chem., Int. Ed. Engl.*, 1971, **10**, 363.
3 P. Werndrup, S. Gohil, V. G. Kessler, M. Kritikos and L. G. Hubert-Pfalzgraf, *Polyhedron*, 2001, **20**, 2163.
4 E. Ilina and V. G. Kessler, *Polyhedron*, 2005, **24**, 3052.
5 M. Hamid, A. A. Tahir, M. Mazhar, M. Zeller, K. C. Molloy and Allen D. Hunter, *Inorg. Chem.*, 2006, **45**, 10457.
6 (*a*) C. Sravani, P. J. Ramakrishna Reddy, O. Md. Hussain and P. J. Readdy, *Solar Energy Soc. India*, 1996, **6**, 1; (*b*) R. Kondo, H. Okhimura and Y. Sakai, *Jpn. J. Appl. Phys.*, 1971, **10**, 1547; (*c*) A. Shiori, Jpn. Patent No. 7, 1997, 909.
7 A. Cybulski, *Catal. Rev. Sci. Eng.*, 1994, **36**, 557.
8 A. A. Mirzaei, H. R. Shaterian, S. H. Taylor and G. J. Hutchings, *Catal. Lett.*, 2003, **87**, 103.
9 G. C. Chinchen and M. S. Spencer, *Catal. Today*, 1991, **10**, 293.
10 (*a*) M. Rehbein, M. Epple and R. D. Fischer, *Solid State Sci.*, 2000, **2**, 473; (*b*) M. Rehbein, R. D. Fischer and M. Epple, *Thermochim. Acta*, 2002, **382**, 143.
11 Y. Guo, R. Weiss and M. Epple, *J. Mater. Chem.*, 2005, **15**, 424.
12 A. Sevin, Y. Hengtai and P. Chaquin, *J. Organomet. Chem.*, 1984, **262**, 391.
13 (*a*) S. J. Tauster, S. C. Fung and L. R. Garten, *J. Am. Chem. Soc.*, 1978, **100**, 170; (*b*) J. P. Belzunegui, J. Sanz and J. M. Rojo, *J. Am. Chem. Soc.*, 1992, **114**, 6749; (*c*) G. Blyholder, *J. Mol. Catal. A: Chem.*, 1997, **119**, 11.
14 B. F. G. Johnson, M. C. Klunduk, T. J. O'Connell, C. McIntosh and J. Ridland, *J. Chem. Soc., Dalton Trans.*, 2001, 1553.
15 G. M. Sheldrick, *Acta Crystallogr., Sect. A: Fundam. Crystallogr.*, 2008, **64**, 112.
16 (*a*) Bruker Advanced X-ray Solutions SMART for WNT/2000 (Version 5.628), Bruker AXS Inc., Madison, Wisconsin, USA, 1997–2002; (*b*) Bruker Advanced X-ray Solutions SHELXTL (Version 6.10), Bruker AXS Inc., Madison, Wisconsin, USA, 2000.
17 M. Shahid, M. Mazhar, P. O' Brien, M. A. Malik and J. Raftery, *Polyhedron*, 2009, **28**, 807.
18 (*a*) K. Nakamoto, *Infrared and Raman Spectra of Inorganic and Coordination Compounds*, Wiley, New York, 4th edn, 1986; (*b*) G. B. Deacon and R. J. Phillips, *Coord. Chem. Rev.*, 1980, **33**, 227.
19 M. Shahid, A. A. Tahir, M. Hamid, M. Mazhar, M. Zeller, K. C. Molloy and A. D. Hunter, *Eur. J. Inorg. Chem.*, 2009, 1043.
20 E. A. Vinogradova, O. Yu. Vassilyeva, V. N. Kokozay, B. W. Skelton, J. K. Bjernemose and P. R. Raithby, *J. Chem. Soc., Dalton Trans.*, 2002, 4248.
21 O. V. Nesterova, A. V. Lipetskaya, S. R. Petrusenko, V. N. Kokozay, B. W. Skelton and J. Jezierska, *Polyhedron*, 2005, **24**, 1425.
22 D. S. Nesterov, V. G. Makhankova, O. Yu. Vassilyeva, V. N. Kokozay, L. A. Kovbasyuk, B. W. Skelton and J. Jezierska, *Inorg. Chem.*, 2004, **43**, 7868.
23 H. P. Walmsley, *Proc. Phys. Soc., London*, 1928, **40**, 7.
24 H. M. Otte, *J. Appl. Phys.*, 1961, **32**, 1536.
25 J. Albertsson, S. C. Abrahams and A. Kvick, *Acta Crystallogr., Sect. B: Struct. Sci.*, 1989, **45**, 34.